COMBINING GROUND-BASED REMOTE SENSING AND BALLOON-BORNE PROFILE MEASUREMENTS IN LINDENBERG (RICHARD-AßMANN-OBSERVATORY) FOR IASI-VALIDATION: METHODS, AVAILABILITY, AND ACCURACY

Bernd Stiller [1], Klemens Barfus [1], Horst Dier [1], Ulrich Görsdorf [1], Ulrich Löhnert [2]
François Montagner [3], Xavier Calbet [3], and Franz H. Berger [1]

(1) Lindenberg Meteorological Observatory / Richard-Aßmann-Observatory, Am Observatorium 12, D-15848 Tauche – OT Lindenberg, Germany
(2) Institute for Geophysics and Meteorology, University of Cologne, Zülpicher Straße 49a, D-50674 Köln, Germany
(3) EUMETSAT, Am Kavalleriesand 31, D-64295 Darmstadt, Germany

Abstract

An Atmospheric Sounding Campaign within the EPS programme in support of the validation of the Infrared Atmospheric Sounding Interferometer (IASI) on board the Metop satellite was performed in Lindenberg from June 01, 2007 to August 31, 2007. A total of 290 radiosondes were launched in addition to the four daily standard radiosoundings. Furthermore measurements with various ground-based remote sensing systems supported the characterization of the state of the atmosphere.

The main task of the campaign was to measure profiles of various meteorological parameters with a high temporal resolution and to subject these measurements an advanced quality control. Besides automated routines the quality control was accomplished by additional investigations of the measurement accuracies of individual instruments and the variability found in the temperature and humidity time series. Some of the results are presented here.

A lot of effort was put into the Integrated Profiling Technique (IPT). The IPT combines radiosoundings and data of microwave profiler, lidar ceilometer and Ka-band radar to an optimal estimate of the current atmospheric state characterized by profiles of temperature, humidity and cloud liquid water content. The application of IPT during the campaign shows that it is an advantageous technique for monitoring temperature and humidity profiles in the boundary layer. However, the combination of several measurements did not always perform in an optimal way due to possible uncertainties of the individual measurement systems.

INTRODUCTION

The main task of the measurement campaign was to provide high quality temperature, humidity and ozone profiles for the validation of the IASI-instrument. The basis of the measurements was formed by additional radiosondes (Vaisala RS92) launched 60 minutes and 5 minutes before each Metop overpass. From June 2007 to August 2007 in total 290 radiosondes were launched in addition to the 368 routine radiosonde ascents at standard times (00, 06, 12, 18 UT).

The quality of the humidity measurements was evaluated by 39 FN-reference soundings (Leiterer et al., 1997; Leiterer et. al., 2005). The Standardized Frequencies (FN) method currently uses a thin-film capacitive polymer sensor of a modified RS90-H Humicap radiosonde. These research humidity reference radiosondes (FN sondes) have been used since the 1990ies to develop a correction method for operational RS80-A Humicap humidity profiles. During the campaign FN-radiosoundings were performed three times a week. Furthermore, three ozone sondes were launched every week.

Instrument / Site	Parameter
Core atmospheric parameters	
Radiosonde RS 92	Vertical profiles of temperature, humidity, wind speed, wind direction and position (coordinates)
Additional atmospheric parameters	
ECC ozone sonde	Vertical profiles of ozone partial pressure
Microwave profiler	Vertical profiles of temperature and humidity
Microwave profiler	Precipitable water vapour
GPS	Precipitable water vapour
Raman lidar	Vertical profiles of water vapour mixing ratio
Brewer	Total column content of ozone
Ka-band radar, ceilometer, radiosonde	Cloud boundaries, including temperature and pressure
Ka-band radar	Radar reflectivity
Integrated Profiling Technique	Vertical profiles of temperature and humidity
Core and additional surface parameters	
Boundary layer field site (GM) Falkenberg	Temperature, humidity, pressure 2 m above ground, wind speed, wind direction 10 m above ground
Pyrgeometer	Outgoing long wave radiation
GCOS Surface Network (GSN) Station Lindenberg	Temperature, humidity, wind, pressure, current weather, precipitation, visibility, clouds
Precision Filter Radiometer	Aerosol optical depth
Whole sky imager	Cloud fraction

Table 1: **Involved measurement systems, instruments, and delivered parameters**

The balloon-borne soundings were supplemented by a variety of ground-based remote sensing. The microwave profiler provided profiles of temperature and humidity. Information of the integrated water vapour was also derived from GPS measurements. A Raman lidar provided profiles of water vapour with high vertical and temporal resolution.

Cloud parameters, e.g. cloud top height, pressure and temperature, were derived by a Ka-band radar and a ceilometer. Cloud cover was determined by human observations and a whole sky imager. A Brewer spectrometer and a precision filter radiometer (PFR) were used for measurements of total ozone and aerosol optical depth, respectively. In-situ measurements of surface meteorological parameters and long wave radiation completed the validation data set of summer 2007 (see Table 1).

DATA AVAILABILITY

Most of the instruments operated reliably so that the data availability was larger than 90 % (Table 2). The complete failure of the Lidar instrument in July and August 2007 did not have consequences for the campaign because in summer season Metop overpassed Lindenberg mostly during daylight and the Lindenberg Raman Lidar has no operational daylight capability. In should be noted that Lidar data provided valuable insight in the variability of humidity for clear sky overpasses in the night during the extension of the campaign in 2008 (see Figure 4).

THE TRUE ATMOSPHERIC STATE

The validation of atmospheric sounding instruments should not be confined to the comparison of the data of the instrument to validate with the reference measurements. Both measurements rather provide a representation of the “true atmospheric state” but include inaccuracies due to the instrument characteristics and measurement principles. The characterization of the “true atmospheric state” forming the base for any validation will succeed if measurement inaccuracies, sampling effects and

No.	System, instrument, parameter	Data availability in days		
		complete	partly available	no data
1	Radiosonde, additional	83	8	1
	Radiosonde, operational	83	9	0
2	ECC Ozone launch 12 UTC (3 per week)	(31)	(0)	(1)
3	Microwave profiler, profiles	88	3	1
4	Microwave profiler, PWV	88	3	1
5	GPS	82	4	6
6	Raman Lidar (RAMSES)	15	31	46
7	Brewer Spectrometer	91	0	1
8	Ka-Band Radar + Ceilometer + Radiosonde	67	20	5
9	Ka-Band Radar	90	1	1
10	IPT	56	28	8
11	Boundary layer field site (GM) Falkenberg	92	0	0
12	Pyrgeometer	91	1	0
13	GSN Station	91	1	0
14	Precision Filter Radiometer	88	0	4
15	Whole Sky Imager	91	0	1

Table 2: **Overview about data availability during atmospheric sounding campaign**

small-scale variability can be identified (e.g. Pougatchev, 2008). Therefore, measurements of the individual instruments should be analyzed with respect to these effects.

The radiosonde, for example, generally provides accurate measurements with a high vertical resolution but it is displaced in the upper troposphere and in the stratosphere. Furthermore, the accuracy of humidity measured by RS92 in low ambient relative humidity is limited.

Ground based lidar measurements allow to derive continuous profiles of humidity in cloud-free conditions but they are limited to the sub-cloud layer when clouds appear. The information included in microwave radiometer profiler data originates mainly from the lower troposphere and is also affected by smoothing effects.

These arguments suggest that there is no single instrument which is capable to characterize the “true atmospheric state” for instrument validation. Consequently the analysis and the combination of various data sources are necessary.

ACCURACY OF BALLOON-BORNE MEASUREMENTS

The vertical resolution of radiosonde measurements is high, but there is a relatively fast passage of the sonde through the atmosphere compared to the characteristic time scales of the turbulence, thus the representativeness of radiosonde measurements is limited.

Furthermore, we should take into account that the radiosonde is drifting away from the location of launch during the ascent. Figure 1 shows (in the left panel) that the average value of the radiosonde drift is larger than 10 km in upper troposphere and it reaches 50 km in stratosphere. It is also remarkable, that the tracks of the first and second sondes of each pair of ascents during a satellite overpass differ in the stratosphere by 5 km in the average and by up to 15 km for individual cases, respectively.

This paper cannot characterize all effects included in radiosonde data and thus we concentrate on selected aspects causing errors and discrepancies.

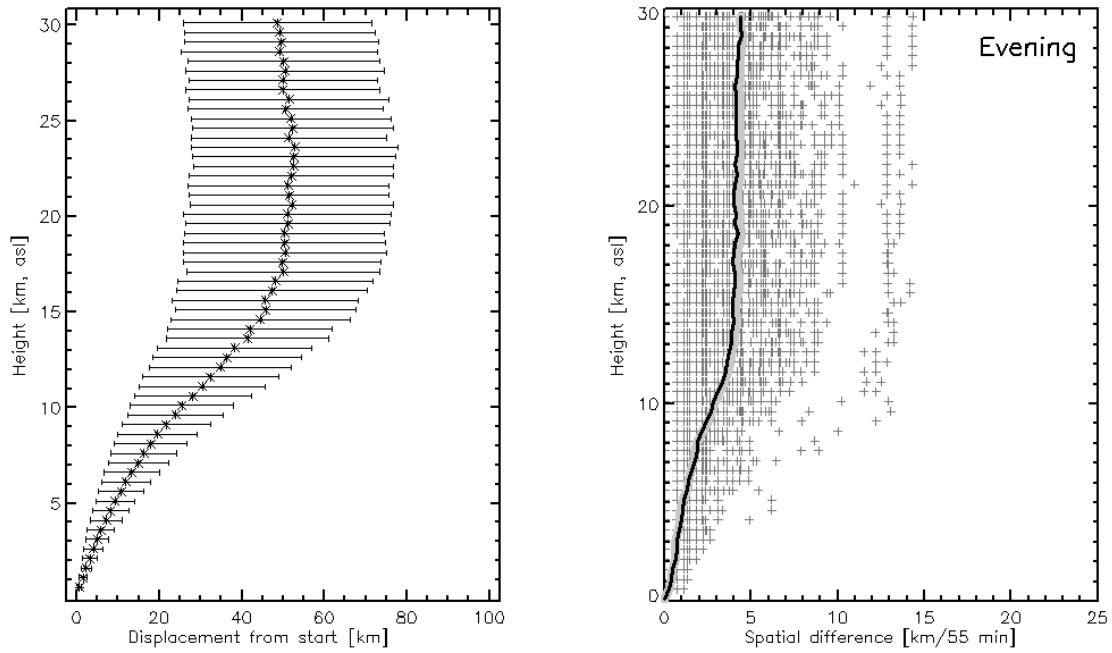

Figure 1: **Mean values and standard deviation of the displacement of the radiosonde during the flight relative to the starting point as a function of height (368 routine and 290 additional ascents in summer 2007, left panel) and spatial differences (single and mean values) between first and second additional ascent (time difference 55 min) for evening overpasses (right panel).**

Figure 2 shows the results of the comparison of humidity measurements during simultaneous ascents of RS92 und RS90-FN reference sondes. There is a random error or instrumental noise of 2 % rH. It is also shown that humidity measurements of the RS-92 standard sonde have a potential bias for lower ambient humidity of up to 4 % rH. Sourtti et al. (2008) showed similar results comparing RS-92 and FN, but analysing the absolute differences between RS-92 and other reference systems like frostpoint hygrometers these deviations appear to be smaller.

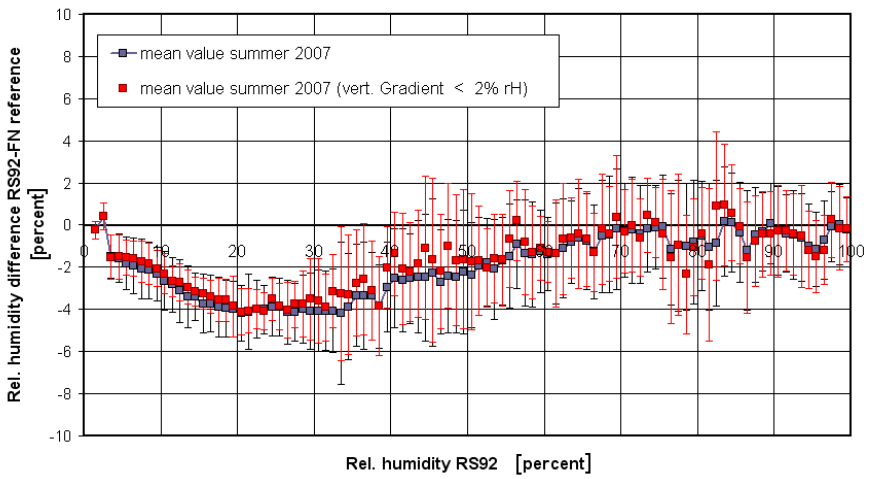

Figure 2: **Results of the comparison of humidity measurements during simultaneous ascents of RS92 und RS90-FN reference sondes (39 FN-reference soundings in summer 2007) in classes of 1 % rH. The y-axis shows the differences between RS92 and RS90-FN as mean value and root mean square difference. To reduce effects of time lag the plot shows supplemental results for differences in cases without distinctive vertical changes of humidity (red squares and lines).**

VARIABILITY

The high repetition rate of radiosoundings (up to 8 ascents per day during the summer campaign) provides valuable insight into the temporal variability of temperature and humidity profiles.

Figure 3 shows the profiles of the mean and the root mean square difference derived from the first and the second additional ascent for the morning overpasses. The average time delay between the two ascents was 55 minutes.

The mean values show increasing temperatures towards the surface due to heating from the ground. The rms difference in the free atmosphere is about 0.6 K. It is slightly larger at the surface (1 K) and near the tropopause region (not shown here). It would be natural to expect an increasing rmsd (increasing temperature und humidity variation) over time scales larger than one hour. This could be proven by tests. Furthermore the rmsd in relative humidity is more prominent than the rmsd for temperature which implies that the troposphere is characterised by more variable humidity-fields. Figure 4 - as an example of Lidar measurements - illustrates pronounced changes of humidity in the lower troposphere and a vertical displacement of a dry layer in a height range between 3 and 4 km.

Pougatchev (2008) has shown that spatial and temporal characteristics of the so-called state non-coincidence error are different at locations with different climates. Lindenberg (humid continental climate) represents a transition regime between tropics and continental midlatitude climate (SGP site).

To characterize underlying processes the series of radiosoundings were used to perform a frequency analysis. Since (due to the sounding schedule) radiosonde time series are unevenly spaced the Lomb-Scargle periodogram was used to detect periodic patterns in the data (Lomb, 1976; Scargle, 1982). Figure 5 shows the prominent frequencies of temperature variations for selected altitudes. Close to the ground frequencies related to the pronounced diurnal cycle in the summer season (1 cycle/day, 2 cycle/day, 3 cycle/day) dominate. In the upper troposphere the signal is mainly composed of low frequencies caused by synoptic changes.

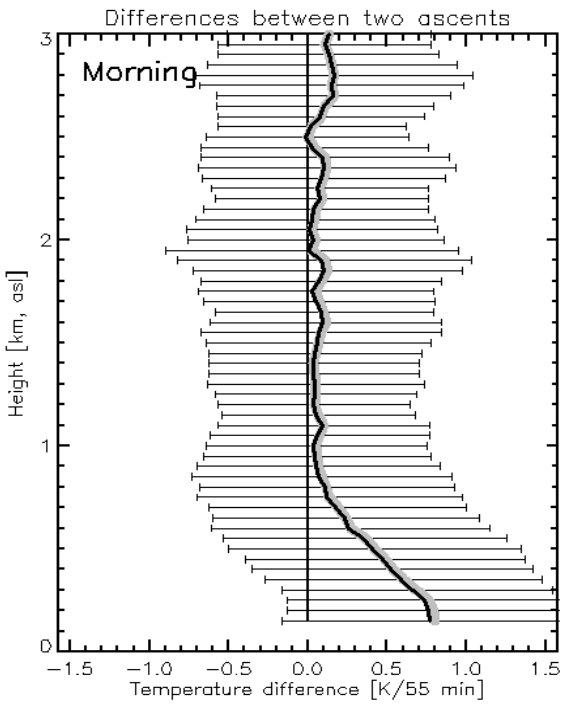

Figure 3: **Mean (black/grey line) temperature differences and root mean square differences between two radiosonde ascents (time delay 55 min) in the morning in summer 2007.**

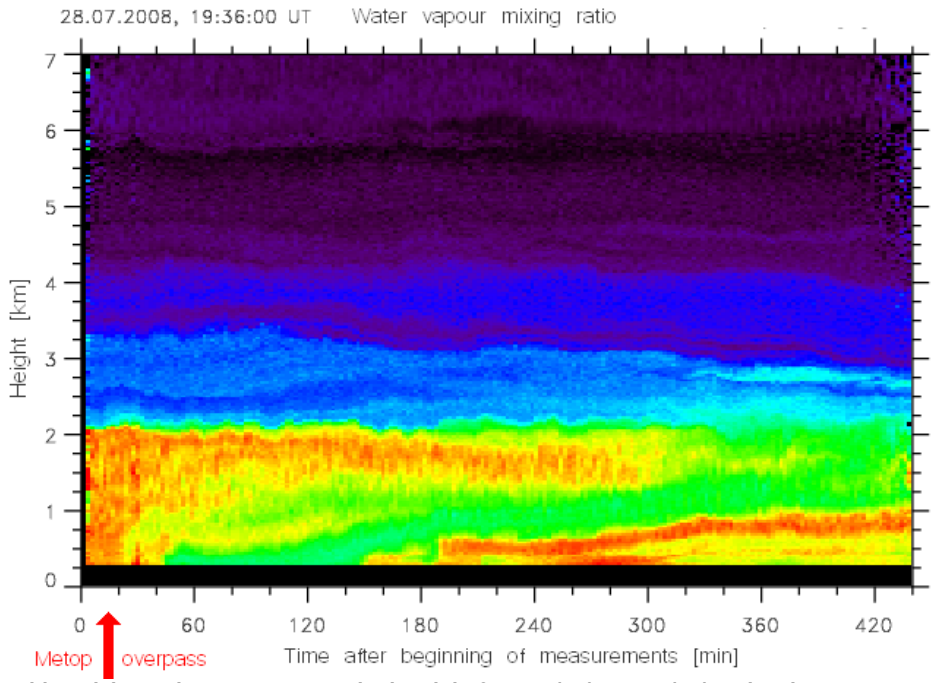

Figure 4: **Lidar mixing ratio measurements in the night from 28/07/08 to 29/07/08 showing pronounced changes of humidity in the lower troposphere and a vertical displacement of a dry layer at a height range between 3 and 4 km. The Lidar data also support the characterisation of variability around the Metop overpass time.**

The diurnal cycle at heights around 30 km and above is caused by heating in the ozone layer.

Additionally an analysis of gravity waves was performed for the summer profiles (an example was shown in the conference presentation). Gravity waves cause temperature changes in the lower stratosphere (LS). On 28/08/07 the temperature amplitude in LS caused by gravity waves exceeds 2 K.

INTEGRATED PROFILING TECHNIQUE (IPT)

The IPT combines radiosoundings and data of a microwave profiler, a lidar ceilometer and a Ka-band radar to an optimal estimate of the current atmospheric state characterized by profiles of temperature,

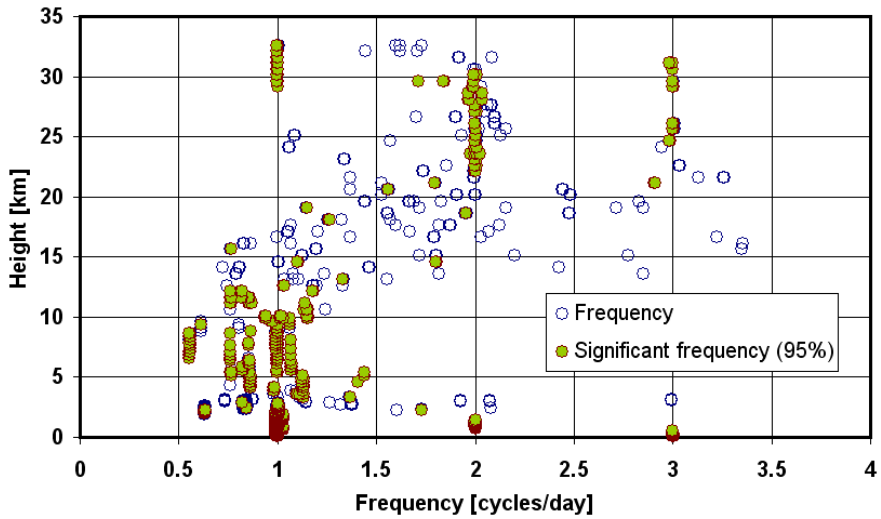

Figure 5: **Prominent frequencies of the Lomb-Scargle-Periodogram of temperature time series from radiosoundings with a repetition rate during summer campaign 2007 at different heights. Significant frequencies are highlighted in green.**

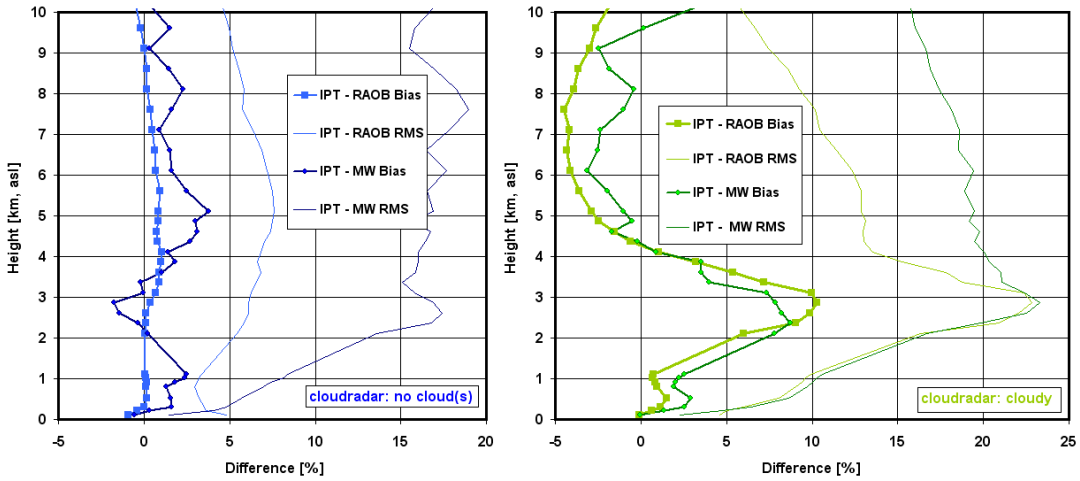

Figure 6: **Averaged differences (bias) and rms differences of atmospheric humidity between combined profile (IPT) and both radiosounding and microwave profiling (left panel: cloud free; right panel: cloudy) during summer campaign 2007**

humidity and cloud liquid water content. This is achieved by an optimal estimation approach (Löhnert et al., 2004) where the relative weight of each measurement is determined by the specified instrument accuracy.

The application of IPT during the campaign shows that it is an advantageous technique for monitoring temperature and humidity profiles in the boundary layer especially if there are no additional radiosoundings.

The IPT makes it possible to quantify the influence of microwave information and radiosoundings to the retrieved (combined) profile. Accurate microwave profiling alone is limited to the lower troposphere, in the upper troposphere (above 3 km) the retrieval accuracy and resolution degrade rapidly (Cimini et. al. 2004).

Therefore almost all IPT temperature profiles are similar to the radiosounding in the upper troposphere. In the case of IPT humidity profiling there are similar results in the upper troposphere just in the case of a cloud free atmosphere (see left panel of Figure 6, N=42762, 66.5% of all cases). But in cloudy cases significant differences occur (Figure 6, right panel). This plot shows the impact of cloud radar information to the humidity profile in the layer where most boundary layer clouds occur between approximately 1500 m and 4000 m. The IPT shows a positive bias of up to 10 percent in rH compared to both radiosoundings and microwave profiling.

This effect of higher humidity in this layer is replicable, but the lower relative humidity of up to 4 percent in rH in the upper troposphere seems to be physically unrealistic. It seems that this effect is not a result of an atmospheric process but rather due to an inconsistency between the different measurements. It is our objective to clarify this point in the future and to look into detail as to which instrument(s) may be responsible for this phenomenon.

SUMMARY / OUTLOOK

Comprehensive datasets for spaceborne sounder validation are available since June 2007. These datasets proved very useful for the validation of temperature, humidity and ozone profiles and also for parameters like cloud-top pressure and cloud-top temperature.

The radiosoundings with a high repetition rate (8 ascents per day during summer campaign) show highly variable humidity-fields in the whole troposphere. These findings are supported by LIDAR-measurements. The high variability of humidity in the lower atmosphere impedes to characterize the

“true atmospheric state“ in a column above the observatory with a diameter close to the instantaneous field-of-view (IFOV) of satellite sounders and size of the ground resolution cell, respectively.

What is the way out? On the one hand, additional measurements (aircraft, drop-sondes, additional remote sensing systems) could support the characterisation of temperature and humidity in an area close to IFOV, for cost reasons this will be a solution for specific field campaigns only. On the other hand, long-term measurements including user-friendly data delivery (as permanent evaluation) will be advantageous.

Further development of the Integrated Profiling Technique (IPT) is needed especially with regard to the inclusion of cloud radar information in the variational technique. Increased efforts have to made to estimate temperature- and humidity-fields, and the statistical parameter like mean value and standard deviation of temperature and humidity, respectively, in an area around Lindenberg.

ACKNOWLEDGEMENTS

The sounding campaign and data evaluation have been supported by EUMETSAT under Contract Nr. (new) EUM/CO/06/4600000259/FM. Thanks to Holger Vömel for helpful discussions about humidity measurements in the stratosphere and to Jens Reichardt for putting actual Lidar measurements at our disposal.

REFERENCES

Cimini, D., Hewison, T. J., Martin, L., Güldner, J., Gaffard, C., and Marzano, F.S. (2006) Temperature and humidity profile retrievals from ground-based microwave radiometers during TUC, Meteorol. Z., **15**, 45-56.

Leiterer, U., Dier, H., and Naebert, T. (1997) Improvements in radiosonde humidity profiles using RS80/RS90 radiosondes of Vaisala. Contrib. Atmos. Phys., **70**, 319–336.

Leiterer, U., Dier, H., Nagel, H., Naebert, T., Althausen, D., Franke, K., Kats, A.., and Wagner, F. (2005) A correction method for RS80-A humicap profiles and their validation by Lidar backscattering profiles in tropical cirrus clouds. J. Atmos. Oceanic Technol., **22**, 18-29.

Löhnert, U., Crewell, S., and Simmer, C. (2004) An integrated approach toward retrieving physically consistent profiles of temperature, humidity, and cloud liquid water. J. Appl. Meteorol., **43**, 1295–1307.

Lomb, N.R. (1976) Least-square frequency analysis of unequally spaced data. Astrophysics Space Science **39**, 447–462.

Pougatchev, N. (2008) Validation of atmospheric sounders by correlative measurements. Appl. Opt. **47**, 4739–4748.

Scargle, J.D. (1982) Studies in astronomical time series analysis. II. Statistical aspects of spectral analysis of unevenly spaced data. The Astrophysical Journal **263**, 835–853.

Suortti, T. M., Kats, A.., Kivi, R., Kämpfer, N., Leiterer, U., Milishevich, L. M., Neuber, R., Paukkunen, A., Ruppert, P., Vömel, H., Yushkov, V. (2008): Tropospheric comparisons of Vaisala radiosondes and balloon-borne frost-point and Lyman-α hygrometers during the LAUTLOS-WAVVAP experiment. J. Atmos. Oceanic Technol., **25**, 149–166.